TISSUE ENGINEERING: Part A
Volume 15, Number 10, 2009

DOI: 10.1089/ten.tea.2009.0150

Original Article

Ti6Ta4Sn Alloy and Subsequent Scaffolding for Bone Tissue Engineering

Yuncang Li, Ph.D., Jianyu Xiong, M.Eng., Cynthia S. Wong, Ph.D.,
Peter D. Hodgson, Ph.D., and Cui'e Wen, Ph.D.

Porous titanium (Ti) and titanium alloys are promising scaffold biomaterials for bone tissue engineering, because they have the potential to provide new bone tissue ingrowth abilities and low elastic modulus to match that of natural bone. In the present study, a new highly porous Ti6Ta4Sn alloy scaffold with the addition of biocompatible alloying elements (tantalum (Ta) and tin (Sn)) was prepared using a space-holder sintering method. The strength of the Ti6Ta4Sn scaffold with a porosity of 75% was found to be significantly higher than that of a pure Ti scaffold with the same porosity. The elastic modulus of the porous alloy can be customized to match that of human bone by adjusting its porosity. In addition, the porous Ti6Ta4Sn alloy exhibited an interconnected porous structure, which enabled the ingrowth of new bone tissues. Cell culture results revealed that human $SaOS_2$ osteoblast-like cells grew and spread well on the surfaces of the solid alloy, and throughout the porous scaffold. The surface roughness of the alloy showed a significant effect on the cell behavior, and the optimum surface roughness range for the adhesion of the $SaOS_2$ cell on the alloy was 0.15 to 0.35 μm. The present study illustrated the feasibility of using the porous Ti6Ta4Sn alloy scaffold as an orthopedic implant material with a special emphasis on its excellent biomechanical properties and *in vitro* biocompatibility with a high preference by osteoblast-like cells.

Introduction

Metallic biomaterials are widely used as load-bearing implants for biomedical applications.[1–7] Human bone tissue accepts some titanium (Ti) alloys well because of their lower elastic modulus,[3–6] superior biocompatibility,[6] and better corrosion resistance than other metals such as SUS316L stainless steel and cobalt-chromium-molybdenum alloy.[8–13] Pure Ti and some of its alloys such as Ti6Al4V and TiNi have been used extensively as load-bearing implants.[2,7,14,15] However, most metallic implant materials including pure Ti and Ti alloys used today are in their solid forms and are often much stiffer than human bone. The elastic modulus of Ti implants ranges from 80 to 130 GPa,[2] which is higher than that of natural bone, which ranges from 0.1 to 30 GPa.[16,17] This mismatch of elastic modulus causes stress shielding, leading to implant loosening and eventual failure.

The elastic modulus of Ti and Ti alloys can be reduced through the introduction of a porous structure.[18–22] Moreover, a porous structure may also provide new bone tissue ingrowth abilities and vascularization.[23–27] Based on the Gibson and Ashby model,[18] the most important structural characteristic of a porous material that influences its elastic modulus is the relative density (ρ/ρ_s), which is measured according to the density of the porous material (ρ) divided by that of the solid material (ρ_s). The elastic modulus of a porous metal is proportional to the product of the elastic modulus of the solid material and the square of its relative density. However, lowering the relative density to meet the requirement of the elastic modulus degrades the plateau stress of the porous material at the same time. The plateau stress of a porous material is proportional to the product of the yield stress of the cell edge material and the relative density to the three-halves power.[18] It is reported that the strength of bone is 42 to 158 MPa in tension and 30 to 323 MPa in compression.[17,28,29] The compressive strength of porous pure Ti with a porosity of 80% is 25 MPa.[27] The strength of porous pure Ti deceases dramatically with the introduction of porosity and is lower than that of natural bone. Therefore, to meet the requirements of low elastic modulus and appropriate strength for implant materials simultaneously, it is necessary to develop new biocompatible Ti alloys that are stronger than those currently available while providing low elastic modulus and adequate strength when it is scaffolding into a porous structure.

In the present study, a new α/β titanium alloy (Ti6Ta4Sn) was designed with the addition of a β stabilizer of tantalum (Ta) and an α stabilizer of tin (Sn). It has been reported that the alloying elements Ta and Sn are biocompatible metals.[30–32]

Institute for Technology Research and Innovation, Deakin University, Geelong, Victoria, Australia.

The new Ti alloy is expected to provide high yield strength because of the addition of Ta and Sn, which ensure the duplex microstructure of the α/β phases.[11,31,32] A porous Ti6Ta4Sn alloy scaffold was prepared using a space-holder sintering method using powder metallurgy. The mechanical properties of the solid and porous alloys were evaluated using compression tests. The *in vitro* biocompatibility of the solid and porous Ti6Ta4Sn alloys was assessed using human $SaOS_2$ osteoblast-like cells and rat fibroblast cells. The feasibility of using the Ti6Ta4Sn scaffold as an orthopedic implant material for bone tissue engineering was examined.

Experimental Materials and Methods

Preparation of solid and porous Ti6Ta4Sn alloy sample

Commercially available elemental metal powders of Ti, Ta, and Sn (all with a purity of 99.8% and particle size of 325 mesh, Atlantic Equipment Engineers, Bergenfield, NJ) were used as starting materials. Elemental metal powders with a nominal composition of Ti6Ta4Sn (in atom percent) were blended for 2 h in a planetary ball milling machine at a weight ratio (balls to powder) of 10:1 and a rotation speed of 100 rpm. The solid alloy samples were prepared by consolidating the mixed metal powder into a green compact at 200 MPa and sintering at 1200°C for 5 h.

To fabricate a porous Ti6Ta4Sn scaffold, the blended Ti6Ta4Sn powder was mixed with ammonium hydrogen carbonate (NH_4HCO_3) particles that were used as the space holder. The mixture of the blended Ti6Ta4Sn powder and the NH_4HCO_3 particles was then cold compacted at a pressure of 200 MPa into green compacts. The compacts were sintered in a vacuum furnace in two steps. The compacts were initially sintered at 175°C for 2 h to burn off the space holder. The temperature was then raised to 1200°C and held for 5 h to sinter the porous structure of the Ti6Ta4Sn alloy. Control of the porosity and pore size were attained by adjusting the initial weight ratio of NH_4HCO_3 to the blended Ti6Ta4Sn powder and the particle size of NH_4HCO_3.

Solid and porous Ti6Ta4Sn alloy disc samples with a diameter of 9 mm and thickness of 2 mm were cut from the sintered products for microstructure and porous structure characterization, phase analysis, and *in vitro* biocompatibility assessments. Cylindrical samples with a diameter of 3 mm and height of 6 mm for the solid alloy and a diameter of 9 mm and height of 15 mm for the porous alloy were used for the compression test to assess mechanical properties.

Microstructure characterization and mechanical property testing

Characterization of the microstructure and phases of the solid Ti6Ta4Sn alloy was performed on a disc sample. The microstructure was observed using optical microscopy, and the porous structure was examined using scanning electron microscopy (SEM). The phases of the Ti6Ta4Sn alloy were analyzed using x-ray diffraction. Disc samples with 6° of surface roughness were prepared using silicon carbide papers with different grits of 80, 240, 600, 800, 1200, and 4000 for investigation of the effect of the surface roughness on the cell behavior. The surface roughness of the disc samples was measured using a surface profilometer (Form Talysurf Intra 112/3477-01, Taylor Hobson Limited, Leicester, United Kingdom). Average surface roughness is defined as the arithmetic mean of the deviation of the protrusions and depressions of the roughness profile from the average line. The surface roughness of the Ti6Ta4Sn alloy discs after grinding with silicon carbide papers of 4000, 1200, 800, 600, 240, and 80 grits were 0.07, 0.11, 0.16, 0.29, 0.43, and 1.69 μm, respectively. To evaluate the mechanical properties of the solid and porous Ti6Ta4Sn alloys, compression tests were performed at room temperature and an initial strain rate of 10^{-3}/s using an Instron universal test machine equipped with a video extensometer (Instron 5567, Norwood, MA).

Cell culture

$SaOS_2$ osteoblast-like cells (a human osteosarcoma cell line with osteoblastic properties) and rat fibroblast cells (Barwon Biomedical Research, Geelong Hospital, Victoria, Australia) were used in the present study. $SaOS_2$ cells were cultured in minimum essential medium (MEM; Gibco, Invitrogen, Australia) supplemented with 10% fetal bovine serum (Bovogen Biologicals, Melbourne, Victoria, Australia), 1% nonessential amino acid (Sigma-Aldrich, Castle Hill, New South Wales, Australia), 10,000 units/ml penicillin-10,000 μg/ml streptomycin (Gibco, Invitrogen, Melbourne, Australia) and 0.4% amphostat B (Invitro, Auckland, New Zealand). The fibroblast cells were cultured in RPMI medium (Gibco, Invitrogen) supplemented with 10% fetal bovine serum (Bovogen Biologicals, Victoria, Australia), 1% of 10,000 U of penicillin, and 10,000 μg/mL of streptomycin (Gibco, Invitrogen). Both cell types were cultured at 37°C in a humidified atmosphere with 5% carbon dioxide CO_2. The culture media were changed every 3 days.

Cytotoxicity tests

The *in vitro* cytotoxicity of the Ti6Ta4Sn alloy samples was assessed from their media extracts obtained based on the international standard ISO10993-5.[33] Before extraction, specimens were sterilized in 70% ethanol for 2 h in an orbital shaker at 150 rpm and air-dried in a biohazard hood at room temperature for 2 h. The specimens were then placed individually in 48-well tissue culture plates (Greiner, Interpath, Victoria, Australia), immersed in MEM at a ratio of 3.6 cm^2/mL (the surface area of disc to volume of medium), and incubated in a humidified atmosphere with 5% CO_2 at 37°C for 3 days. The discs were removed from the medium to obtain the extracts of Ti6Ta4Sn alloy.

$SaOS_2$ cells and rat fibroblast cells were separately seeded in the different extracts, each at a density of 10,000 cells per well. Cells were also seeded in the wells containing only the medium and incubated for 3 days as a negative control. After 5 days of culture, cells were harvested using 0.1% trypsin-5 mM ethylenediaminetetraacetic acid (Sigma-Aldrich) and collected. Cell counts were obtained using the trypan blue exclusion method,[34] whereby dead cells were stained blue and live cells remained clear. The cell viability was determined according to the ratio of live cells to the total number of cells per sample.

Cell proliferation assay

$SaOS_2$ cell proliferation and the density of cell attachment on the solid Ti6Ta4Sn samples were evaluated using

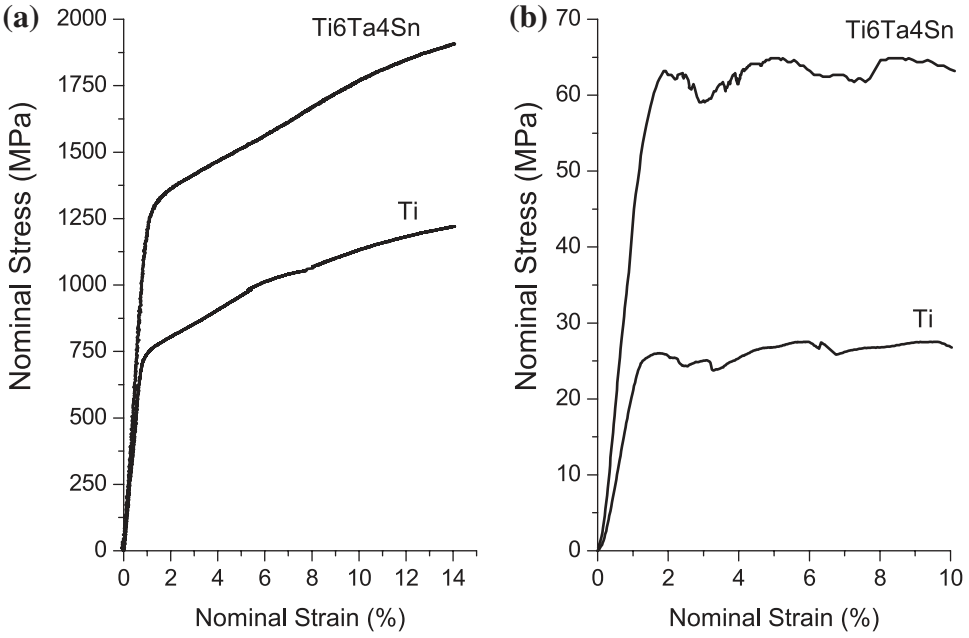

FIG. 1. Nominal stress-strain curves: (**a**) solid Ti6Ta4Sn and titanium (Ti); (**b**) porous Ti6-Ta4Sn scaffold and porous pure Ti scaffold with the same porosity of 75%.

3-(4, 5-dimethylthialzol-2-yl)-2, 5-diphenyltetrazolium bromide (MTT) assay.[35] The assay is dependent on the cellular reduction of MTT (Sigma-Aldrich), by the mitochondrial dehydrogenase of viable cells, to a blue formazan product that can be measured using a spectrophotometer. Briefly, 7 days after cell culture, Ti6Ta4Sn discs were transferred into new 48-well plates. MTT solution (5 mg/mL) was added to each well in plates without and with discs and incubated for 4 h at 37°C. The formazan was then solubilized with acidified isopropanol (0.04 N of hydrochloric acid in isopropanol). Optical density was measured using a spectrophotometer (GENios Pro, Tecan, Mannedorf, Switzerland) at 570 nm. Wells and Ti6Ta4Sn discs incubated with medium alone were used as negative controls. A standard curve of known viable cell numbers was used to calculate viable cell numbers for each condition.

Cell morphology observation

The cell morphology of the $SaOS_2$ osteoblast-like cells on surfaces of the solid Ti6Ta4Sn discs was observed using a confocal microscope (Leica SP5, Leica Microsystems, Wetzlar, Germany) and SEM (Leica 440, Leica Microsystems). For confocal microscopy observation, after cell culture, the cell-seeded discs were fixed in 2% paraformaldehyde and permeabilized with 0.2% (v/v) triton-X100 in phosphate buffered saline (PBS; Sigma-Aldrich) each for 10 min at room temperature. The discs were then incubated with 1% phalloidin and 4′-6-diamidino-2-phenylindole (DAPI) overnight at 4°C. The discs were washed three times with PBS between each of the steps mentioned above. The stained samples were stored in PBS until required, and confocal microscopy observations of these samples were conducted within 1 week of staining. For SEM observation, after cell culture, the cell-seeded discs were fixed in 3.9% glutaraldehyde for 12 hrat room temperature. Then the cells were dehydrated through sequential washings in 60%, 70%, 80%, 90%, 95%, and 100% ethanol solutions for 10 min at each step. After that, the samples were chemically dried using hexamethyldisilazane[36] and coated in gold for SEM observations.

In the present study, all cell culture experiments were conducted in triplicate and results were expressed as means ± standard deviations. One-way analysis of variance (SPSS 14.0 for Windows software, SPSS, Inc., Chicago, IL) was applied to determine the statistical significance of the differences observed between groups. $P < 0.05$ was considered to be statistically significant.

Results and Discussion

Mechanical properties and microstructure of Ti6Ta4Sn alloy

The mechanical properties of the solid Ti6Ta4Sn alloy were evaluated using a compression test. For comparison, the compressive properties of pure Ti were also tested. The nominal stress–strain curves of the Ti6Ta4Sn alloy and pure Ti are shown in Figure 1a. The solid Ti6Ta4Sn alloy exhibited a yield strength of 1250.2 MPa and an elastic modulus of 115.2 GPa. It can be seen that the yield strength of the Ti6-Ta4Sn alloy is significantly higher than that of pure Ti (720 MPa), and the elastic modulus of the solid Ti6Ta4Sn alloy is slightly higher than that of pure Ti (105 GPa) and significantly higher than that of natural bone (0.1 ~ 30 GPa).[17,29] This set of mechanical properties of the solid Ti6Ta4Sn alloy necessitates the scaffolding processing of the alloy.

The nominal stress–strain curves of the porous Ti6Ta4Sn alloy and pure Ti are shown in Figure 1b. The plateau stress and elastic modulus of the porous Ti6Ta4Sn alloy with a porosity of 75% were approximately 62.0 MPa and 4.6 Gpa, respectively; the pure Ti sample with a porosity of approximately 75% exhibited a plateau stress and elastic modulus of 25.0 MPa and 2.9 GPa, respectively. It can be seen that the plateau stress of the porous Ti6Ta4Sn alloy is significantly higher than that of pure Ti with the same porosity level. The

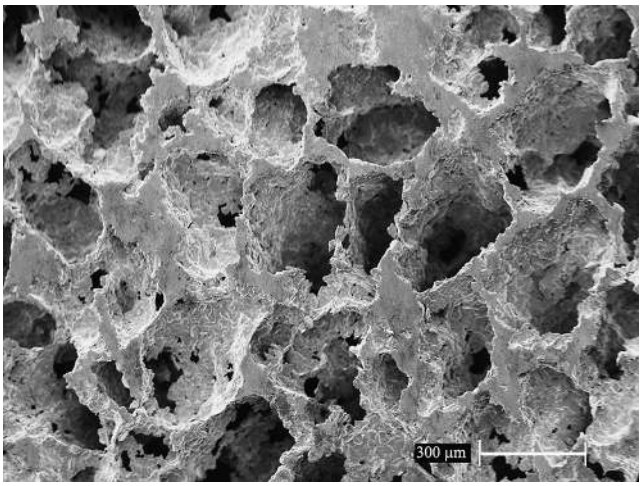

FIG. 2. Scanning electron microscopy (SEM) micrograph of a porous Ti6Ta4Sn alloy with a porosity of 75%.

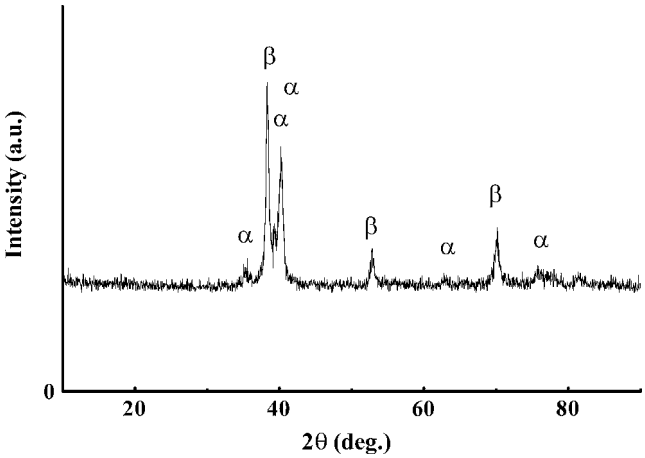

FIG. 4. X-ray diffraction patterns of the Ti6Ta4Sn alloys.

strength and the elastic modulus of the Ti6Ta4Sn with a porosity of 75% are close to those of natural bone.[17,29] Moreover, the mechanical properties of a porous metal can be tailored to mimic those of natural bone by altering the level of porosity.[18–27,37,38] Therefore, the mechanical properties of porous Ti6Ta4Sn can be customized to meet the specific requirements of the implant material where it is needed.

The SEM micrograph of Ti6Ta4Sn alloy with a porosity of 75% is shown in Figure 2. The porous Ti6Ta4Sn alloy exhibited an interconnected porous structure with open pores. This feature is important because an interconnected open-cell porous structure allows new bone tissue ingrowth and body fluid transportation. The pore size of the porous Ti6Ta4Sn alloy ranged from 200 to 500 μm. This pore size range is tailored to impart the porous Ti6Ta4Sn scaffold with new bone tissue ingrowth ability.[20–27]

The microstructure of the solid Ti6Ta4Sn alloy was observed using optical microscope, and the phases were analyzed using x-ray diffraction. The microstructure of the Ti6Ta4Sn alloy is shown in Figure 3. The Ti6Ta4Sn alloy exhibited a typical duplex microstructure consisting of α and β phases. α/β Ti alloys possess good comprehensive properties, including high yield strength, excellent corrosion resistance, and good fracture toughness.[1–7] The x-ray diffraction pattern of the alloy is shown in Figure 4. Diffraction peaks attributable to α and β phases from the pattern confirmed a duplex microstructure. This result is consistent with the microstructural observation.

Cytotoxicity of Ti6Sn4Sn

Another factor that plays an important role in ensuring a successful implant material is the biocompatibility. To assess the biocompatibility of the Ti6Ta4Sn alloy, *in vitro* assessments were performed on the extract of the Ti6Ta4Sn alloy using human $SaOS_2$ osteoblast-like cells and rat fibroblast cells.

Proliferations for $SaOS_2$ osteoblast-like cells and fibroblast cells were observed on the Ti6Ta4Sn alloy discs. Figure 5 shows the cell viabilities of the $SaOS_2$ osteoblast-like cells and fibroblast cells after culture for 5 days in the medium pre-

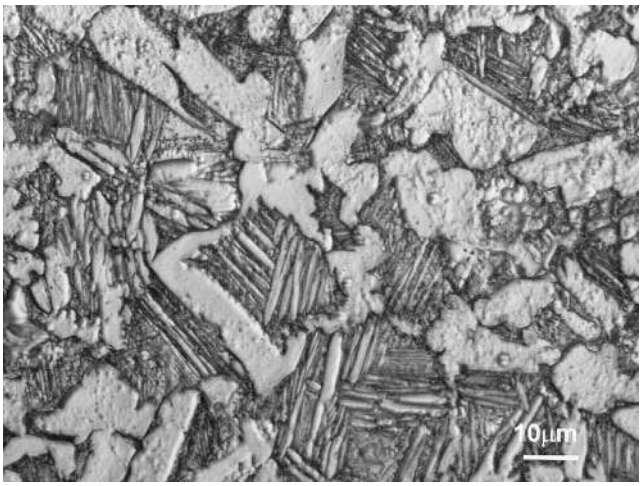

FIG. 3. Microstructure of the Ti6Ta4Sn alloy showing a duplex microstructure of α/β phases.

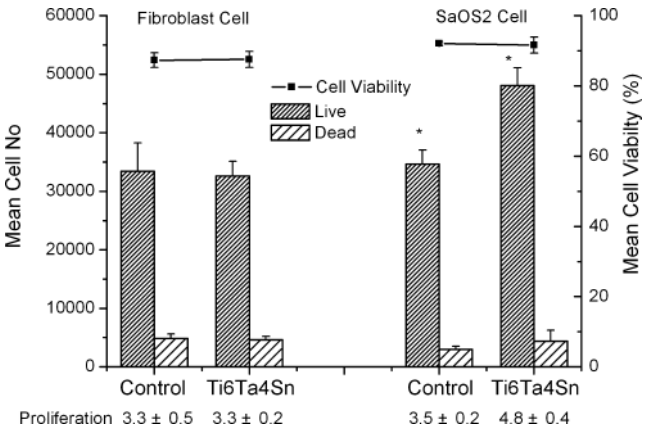

FIG. 5. Cell viabilities of $SaOS_2$ cells and fibroblast cells after culture for 5 days in medium preconditioned with the Ti6Ta4Sn alloy ($^*p < 0.05$).

conditioned with the Ti6Ta4Sn alloy. For the fibroblast cells, the proliferation of the control group was 3.3 times the initial amount, and that of the Ti6Ta4Sn alloy group was also 3.3 times the initial amount. The viabilities of the control group and the alloy group were 87.3% and 87.6%, respectively. On the other hand, the proliferation of SaO_2 cells in the control group was 3.5 times the initial amount, and that of the Ti6Ta4Sn alloy group was 4.4 times the initial amount. The viabilities of the control group and the alloy group were 91.6% and 92.0%, respectively. The cell viability of the Ti6Ta4Sn alloy group was similar to that of the control group for both types of cells, which means it had excellent biocompatibility. It can be concluded that the Ti6Ta4Sn alloy is nontoxic and of excellent biocompatibility.

The cell proliferations were similar in the control groups for osteoblast-like cells and fibroblast cells (3.5 times) (Fig. 5). However, the cell proliferation was better for the osteoblast-like cells (4.8 times) than the fibroblast cells (3.5 times) in the alloy group. The $SaOS_2$ osteoblast-like cells showed higher proliferation than the fibroblast cells on the Ti6Ta4Sn alloy. The proliferation rate of the fibroblast cells demonstrated that the Ti6Ta4Sn alloy is biocompatible and may minimize the formation of fibrous encapsulation between host tissue and implant. Lower fibroblast adhesion and greater osteoblast adhesion on implants are critical criteria for a successful enthesis tissue engineering material.[39–47] This feature is of great significance because the new alloy is designed for orthopedic implant materials.

Effect of surface roughness on the cell adhesion and proliferation

In the present study, MTT assay to assess cell proliferation was performed on the solid Ti6Ta4Sn alloy with different surface roughnesses to determine the effect of surface roughness on the cell behavior of $SaOS_2$ osteoblast-like cells. Cells that have attached and grown on the surface of the control well, cell-seeded alloy discs, and the wells that were used to contain the discs were counted. "Disc + Well" refers to the sum of the cell numbers of seeded discs and their respective wells. The cell proliferation on the Ti6Ta4Sn alloy surfaces with different roughnesses are shown in Figure 6. There was little variation in cell numbers on the surface of wells that contain the alloy discs with different roughnesses, although the surface roughness of the Ti6Ta4Sn alloy significantly affected the number of cells that attached and grew on the alloy discs ($p < 0.05$), as shown in Figure 7. The alloy discs with a surface roughness between 0.15 and 0.35 μm showed an excellent cell proliferation rate (>180 cell/mm^2). The optimal surface roughness ranged from 0.15 to 0.35 μm for osteoblast cell adhesion and proliferation, peaking at 0.2 μm, as shown in Figure 7.

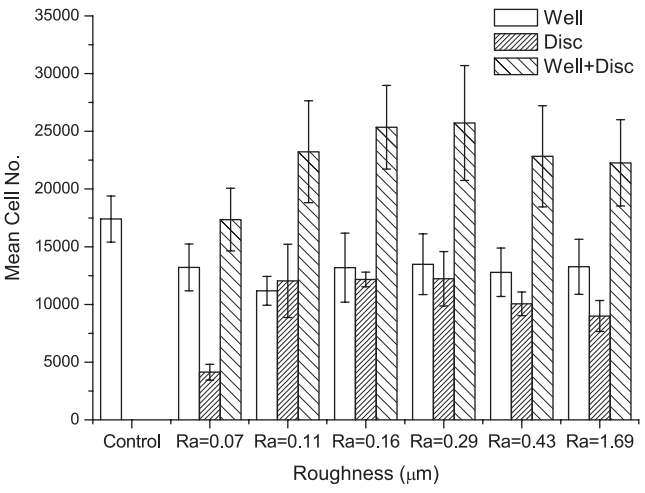

FIG. 6. Cell proliferation of the $SaOS_2$ cells on the solid Ti6Ta4Sn alloy surfaces with different roughness (Well + Disc refers to the sum of the cell numbers seeded on the alloy discs and their respective wells).

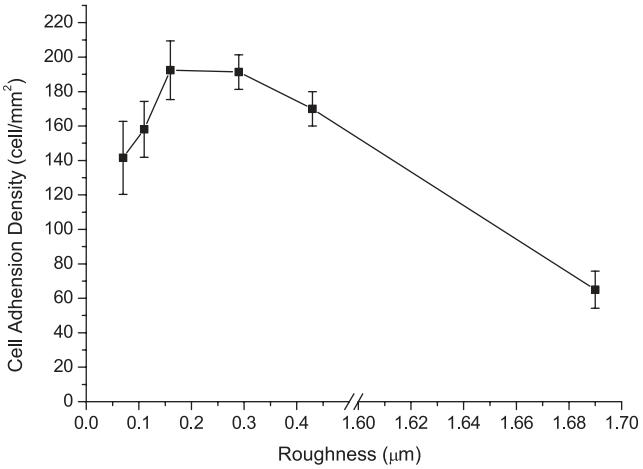

FIG. 7. Adhesion density of $SaOS_2$ cells on the surface of the Ti6Ta4Sn alloy with the different roughness after culture for 7 days.

The ability of cells to attach and spread on Ti-based alloy surfaces is a crucial parameter in implant technology. Surface properties, such as composition, roughness, and texture of the implant, greatly affect cellular behavior, proliferation, and differentiation.[48–50] Deligianni *et al.*[51] investigated the effect of surface roughness of hydroxyapatite on human bone marrow cell adhesion, proliferation, differentiation, and detachment strength. They found that proliferation rates were significantly lower on hydroxyapatite than on culture plate for all surface roughness values tested, and cell adhesion, proliferation, and detachment strength were sensitive to surface roughness and were greater with greater surface roughness (0.73–4.68 μm).

Cell morphology observations

The SEM micrographs of $SaOS_2$ osteoblast-like cells on the solid and porous Ti6Ta4Sn alloy after 7 days of culture are shown in Figure 8. $SaOS_2$ cells attached, spread, and grew well on the surfaces of the solid Ti6Ta4Sn alloy with a surface roughness of 0.16 μm, as shown in Figure 8a. Figure 8b shows the cell morphologies at higher magnification to provide a closer observation of cell adhesion and spreading. Cells on the porous Ti6Ta4Sn alloy were observed to spread well, both on the edges of porous scaffold and inside the pores, as shown in Figure 8c and d. The $SaOS_2$ cells grew over the pores, bridging the pore edges (Fig. 8d). Extracellular matrix

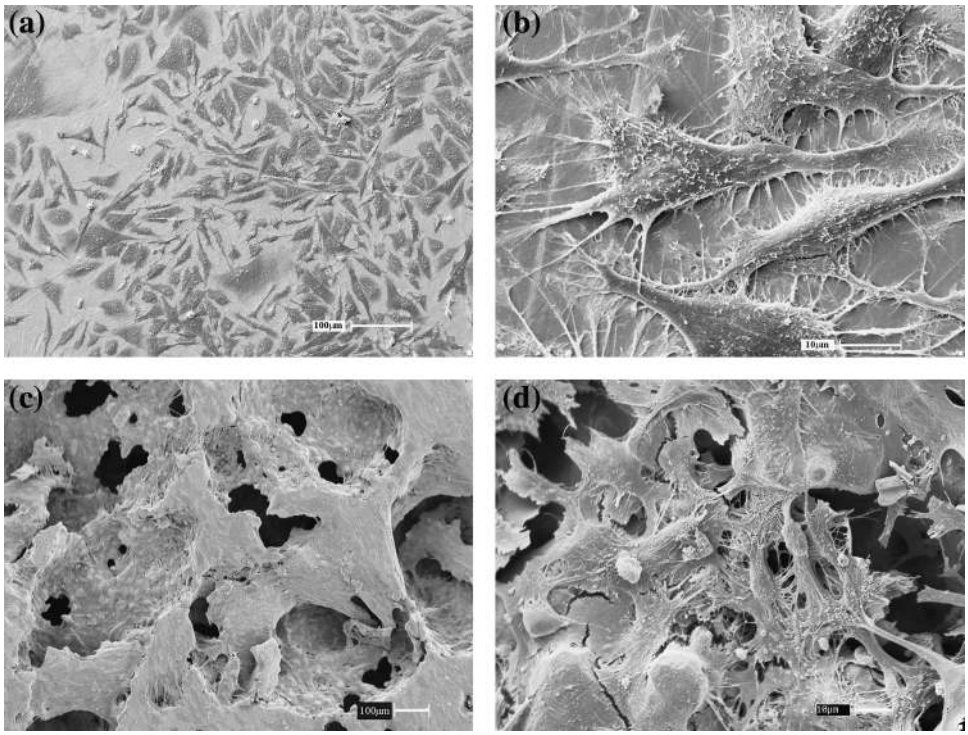

FIG. 8. SEM images showing $SaOS_2$ cells attachment on the solid (**a**) with low magnification and (**b**) with high magnification and porous Ti6Ta4Sn discs (**c**) with low magnification and (**d**) with high magnification after cell culture for 7 days.

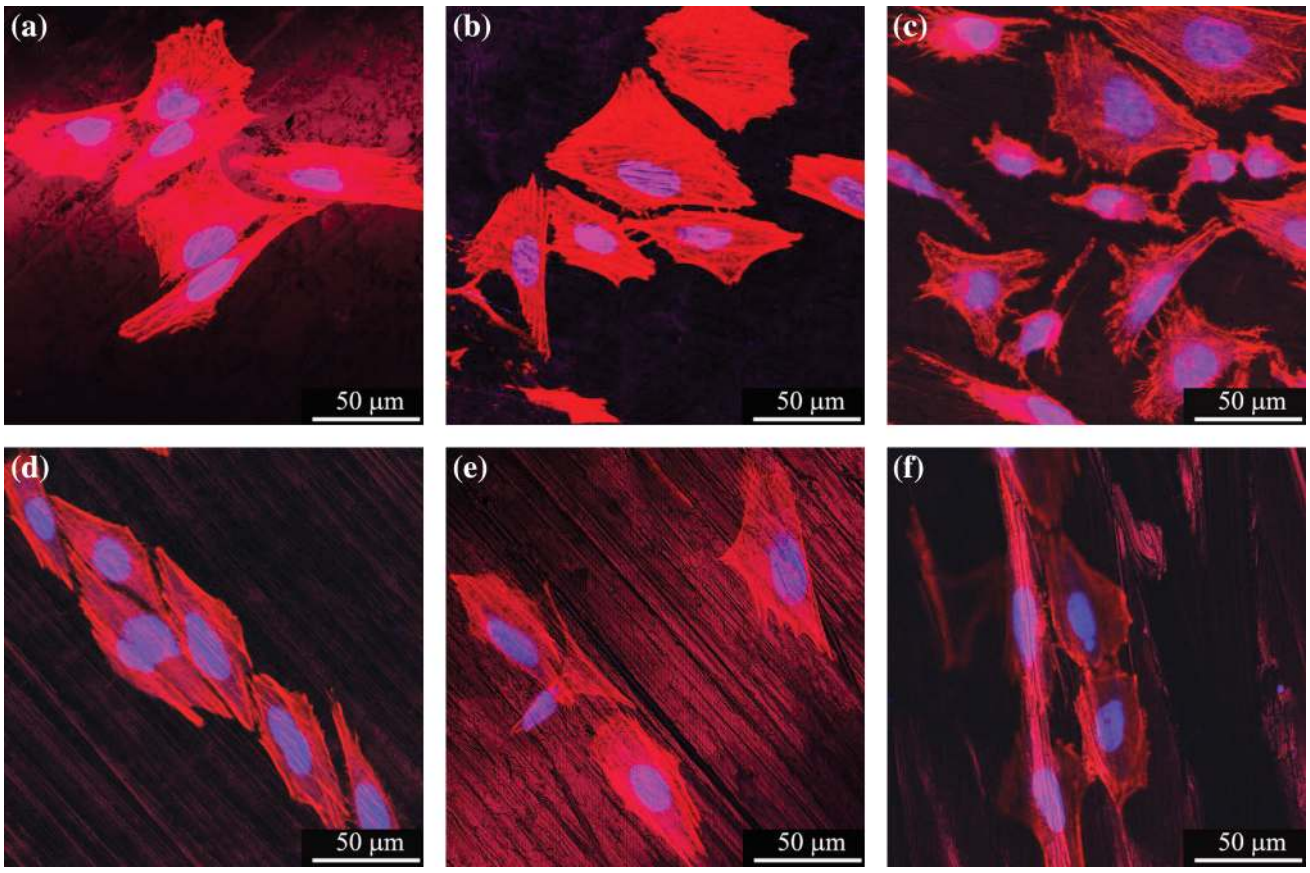

FIG. 9. Confocal images showing $SaOS_2$ cells attachment on the Ti6Ta4Sn alloy surfaces with different roughnesses: (**a**) 0.07 μm, (**b**) 0.11 μm, (**c**) 0.16 μm, (**d**) 0.29 μm, (**e**) 0.43 μm, and (**f**) 1.69 μm. Color images available online at www.liebertonline.com/ten.

formation can also be found on the surface of the solid and porous Ti6Ta4Sn alloy. These results indicate that the Ti6Ta4Sn alloy exhibited good biocompatibility. The results of the cell morphology and attachment observation are consistent with the results of the cytotoxicity assay.

Meanwhile, the $SaOS_2$ cells displayed different adhesion and proliferation behaviors on the Ti6Ta4Sn alloy surfaces with varying roughness. Figure 9 shows cell morphologies and densities on the alloy surface with roughnesses of (Fig. 9a) 0.07, (Fig. 9b) 0.11, (Fig. 9c) 0.16, (Fig. 9d) 0.29, (Fig. 9e) 0.43, and (Fig. 9f) 1.69 μm. Cell culture on the alloy surface with roughness of 1.69 μm grew and spread along the protruding strips with a claviform shape along the grinding grooves (Fig. 9f). For the cells seeded onto the alloy surface with lower roughness (0.11–0.43 μm), cells grew and spread in all directions, and cell adhesion was improved as more cells attached on the surface (Fig. 9b–e). Although the alloy surface with the smallest roughness (0.07 μm) showed less cell attachment, cells grew and spread on the alloy surface in all directions (Fig. 9a. The surface with lower roughness showed lower cell adhesion. Surface roughness significantly affected cell attachment and proliferation.

Boyan and Schwartz[52] indicated that osteoblasts displayed a flattened fibroblastic morphology when they were cultured on a smooth surface (<0.2 μm, with the distance between peaks > the length of the cell). If the surface roughness was smaller than 2 μm and the distance between peaks was less than the length of the cell, the cells were unable to flatten and spread. The cells anchored on the surface via focal attachments by cytoplasmic extensions to multiple peaks. This forced the cell to assume a more osteoblastic morphology. Chen *et al.*[53] indicated that micro-grooved surfaces with depths of approximately 10 μm, widths of 11 μm, and spacings of 20 μm provided the best combination of cell orientation and adhesion of human osteosarcoma cells to a laser-textured Ti6Al4V surface. In the present study, cell culture results indicated an optimum surface roughness range for the adhesion of $SaOS_2$ cell on the Ti6Ta4Sn alloy. It can be concluded that surface roughness of an implant material has a significant influence on cell adhesion and proliferation for the newly designed Ti6Ta4Sn alloy. The cell morphology and attachment observations confirms the MTT assay results described above. Postiglione *et al.*[54] and Saldana *et al.*[55] have also reported similar results.

Conclusion

A new Ti6Ta4Sn alloy for orthopedic implant materials has been developed and investigated. The new alloy exhibited an α/β duplex-phase microstructure and possessed the high yield strength of 1250.2 MPa and an elastic modulus of 115.2 GPa. The new alloy was further scaffolded into a porous structure through a special powder metallurgical process, which included the burn-off of a space-holder material. The porous Ti6Ta4Sn alloy scaffold with a porosity of 75% displayed an interconnected porous structure, as well as mechanical properties close to those of natural bone. The pore size of the porous alloy ranged from 200 to 500 μm. $SaOS_2$ osteoblast-like cells and rat fibroblast cells were used to assess the *in vitro* biocompatibility of the new solid and porous Ti6Ta4Sn alloys. Results indicated that the new alloy and its porous scaffold possessed excellent biocompatibility, with a high preference for osteoblast-like cells. Surface roughness was also found to affect cell adhesion and proliferation significantly. There was an optimum surface roughness range (0.15–0.35 μm) that the $SaOS_2$ osteoblast-like cells preferred to attach, grow, and spread on the alloy. The new Ti6Ta4Sn alloy scaffold had excellent mechanical properties, new bone tissue ingrowth abilities, and excellent biocompatibility.

Acknowledgments

The authors acknowledge the financial support for this research through the Australian Research Council (ARC) Discovery Project DP0770021. Peter Hodgson is also supported by the ARC through a Federation Fellowship.

Disclosure Statement

The authors have no competing financial interests.

References

1. Wang, K. The use of titanium for medical applications in the USA. Mater Sci Eng A **213**, 134, 1996.
2. Long, M., Rack, H.J. Titanium alloys in total joint replacement—a materials science perspective. Biomaterials **19**, 1621, 1998.
3. Niinomi, M. Recent metallic materials for biomedical applications. Metal Mater Trans **33A**, 477, 2002.
4. Rack, H.J., Qazi, J.I. Titanium alloys for biomedical applications. Mater Sci Eng C **26**, 1269, 2006.
5. Sakaguchi, N., Niinomi, M., Akahori, T., Takeda, J., Toda, H. Relationship between tensile deformation behavior and microstructure in Ti-Nb-Ta-Zr. Mater Sci Eng C **25**, 363, 2005.
6. Niinomi, M., Akahori, T., Takeuchi, T., Katsura, S., Fukui, H., Toda, H. Mechanical properties and cyto-toxicity of new beta type titanium alloy with low melting points for dental applications. Mater Sci Eng C **25**, 417, 2005.
7. Williams, D.F. Titanium and Titanium Alloys, Biocompatibility of Clinical Implant Materials. Florida: CRC Press Inc., 1982.
8. Kim, Y.M, Takadama, H., Kokubo, T., Nishiguchi, S., Nakamura, T. Formation of a graded bioactive surface structure on Ti-15Mo-5Zr-3Al alloy by chemical treatment. Biomaterials **21**, 353, 2000.
9. Wack, T., Biehl, V., Breme, J., Schwanke, C., Schaeffer, L. Dental implants of TiTa30 produced by powder technology. Mater Sci Forum **299–300**, 348, 1999.
10. Niinomi, M. Mechanical properties of biomedical titanium alloys. Mater Sci Eng A **243**, 231, 1998.
11. Okazaki, Y., Ito, Y. New Ti alloy without Al and V for medical implant. Adv Eng Mater **2**, 278, 2000.
12. Zhou, Y.L., Niinomi, M., Akahori, T., Fukui, H., Toda, H. Corrosion resistance and biocompatibility of Ti-Ta alloys for biomedical applications. Mater Sci Eng A **398**, 28, 2005.
13. Gunawarman, Niinomi, M., Akahori, T., Souma, T., Ikeda, M., Toda, H., Terashima, K. Fatigue characteristics of low cost β titanium alloys for healthcare and medical applications. Mater Trans **46**, 1570, 2005.
14. Li, B.Y., Rong, L.J., Li, Y.Y., Gjunter, V.E. Synthesis of porous Ni-Ti shape-memory alloys by self-propagating high-temperature synthesis: reaction mechanism and anisotropy in pore structure. Acta Mater **48**, 3895, 2000.
15. Chu, C.L., Chung, C.Y., Zhou, J., Pu, Y.P., Lin, P.H. Fabrication and characteristics of bioactive sodium

titanate/titania graded film on NiTi shape memory alloy. J Biomed Mater Res A **75**, 595, 2005.
16. Wang, X.J., Li, Y.C., Hodgson, P.D., Wen, C.E. Nano- and macro-scale characterisation of the mechanical properties of bovine bone. Mater Forum **31**, 156, 2007.
17. Currey, J.D. Bones structure and mechanics, 2nd Ed. Princeton, NJ: Princeton University Press, 2006.
18. Gibson, L.G., Ashby, M.F. Cellular Solids: Structure and Properties. Cambridge, UK: Cambridge University Press, 1997.
19. Banhart, J. Manufacture, characterisation and application of cellular metals and metal foams. Prog Mater Sci **46**, 559, 2001.
20. Wen, C.E., Mabuchi, M., Yamada, Y., Shimojima, K., Chino, Y., Asahina, T. Processing of biocompatible porous Ti and Mg. Scr Mater **45**, 1147, 2001.
21. Dunand, D. Processing of titanium foams. Adv Eng Mater **6**, 369, 2004.
22. Bram, M., Stiller, C., Buchkremer, H.P., Stover, D., Baur, H. High-porosity titanium, stainless steel, and superalloy parts. Adv Eng Mater **2**, 196, 2000.
23. Alvarez, K., Sato, K., Hyun, S.K., Nakajima, H. Fabrication and properties of lotus-type porous nickel-free stainless steel for biomedical applications. Mater Sci Eng C **28**, 44, 2008.
24. Alvarez, K., Hyuna, S-K, Nakano, T., Umakoshi, Y., Nakajima, H. In vivo osteocompatibility of lotus-type porous nickel-free stainless steel in rats. Mater Sci Eng C **29**, 1182, 2008.
25. Sargeant, T.D., Guler, M.O., Oppenheimer, S.M., Mata, A., Satcher, R.L., Dunand, D.C. Stupp, S.I. Hybrid bone implants: self-assembly of peptide amphiphile nanofibers within porous titanium. Biomaterials **29**, 161, 2008.
26. Wen, C.E., Yamada, Y., Shimojima, K., Chino, Y., Asahina, T., Mabuchi, M. Processing and mechanical properties of autogenous titanium implant materials. J Mater Sci Mater Med **13**, 397, 2002.
27. Wen, C.E., Yamada, Y., Shimojima, K., Chino, Y., Hosokawa, H., Mabuchi, M. Novel titanium foam for bone tissue engineering. J Mater Res **17**, 2633, 2002.
28. Thomson, R.C., Wake, M.C., Yaszemski, M.J., Mikos, A.G. Biodegradable polymer scaffolds to regenerate organs. Adv Polym Sci **122,** 245, 1995.
29. Evans, F.G., Lissner, H.R. Tensile and compressive strength of human parietal bone. J Appl Physiol **10**, 493, 1957.
30. Steinemann, S.G. Corrosion of surgical implants—in vivo and in vitro tests. In: Winter, G.D., Leray, J.L., De Goot, K., eds. Evaluation of Biomaterials, Advances in Biomaterials. Chichester: Wiley, 1980, pp. 1–34.
31. Okazaki, Y., Rao, S., Tateishi, T., Ito, Y. Cytocompatibility of various metal and development of new titanium alloys for medical implants. Mater Sci Eng A **243**, 250, 1998.
32. Niinomi, M. Fatigue performance and cyto-toxicity of low rigidity titanium alloy, Ti-29Nb-13Ta-4.6Zr. Biomaterials **24**, 2673, 2003.
33. Biological Evaluation of Medical Devices. Part 5: Test for *in vitro* cytotoxicity. International Organization for Standardization, ANSI/AAMI, Arlington, VA, 1999.
34. Kruse, P.F., Patterson, M.K. Tissue Culture, Methods and Application. New York: Academic Press, 1973.
35. Mosmann, T. Rapid colorimetric assay for cellular growth and survival: application to proliferation and cytotoxicity assays. J Immunol Methods **65**, 55, 1983.
36. Bray, D.F., Bagu, J., Koegler, P. Comparison of hexamethyldisilazane (HMDS), peldri 11, and critical-point drying methods for scanning electron microscopy of biological specimens. Microsc Res Tech **26**, 489, 1993.
37. Xiong, J.Y., Li, Y.C., Hodgson, P.D., Wen, C.E. TiNi shape memory alloy foams synthesized by spacer sintering and their properties. J Mater Sci Eng **26**, 892, 2007.
38. Itin, V.I., Gyunter, V.E., Shabalovskaya, S.A., Sachdeva, R.L.C. Mechanical properties and shape memory of porous nitinol. Mater Characterization **32**, 179, 1994.
39. Davies, J.E., Hosseini, M.M. Bone formation and healing. In: Davies, J.E., ed. Bone Engineering. Toronto, Cananda: em squared incorporated, 2000. pp. 1–14.
40. Dee, K.C., Puleo, D.A., Bizios, R. An Introduction to Tissue-Biomarterial Interactions. Hoboken, NJ: John Wiley & Sons, Inc., 2002.
41. Brunette, D.M., Chehroudi, B. The effect of surface topography of micromachined titanium substrata on cell behaviour in vitro and in vivo. J Biomech Eng **121**, 49, 1999.
42. Wang, I-NE., Shan, J., Choi, R., Oh, S., Kepler, C.K., Chen, F.H., Lu, H.H. Role of osteoblast-fibroblast interactions in the formation of the ligament-to-bone interface. J Orthop Res **25**, 1609, 2007.
43. Vance, R.J., Miller, D.C., Thapa, A., Haberstroh, K.M., Webster, T.J. Decreased fibroblast cell density on chemically degraded poly-lactic-co-glycolic acid, polyurethane, and polycaprolactone. Biomaterials **25**, 2095, 2004.
44. Smith, L.L., Niziolek, P.J., Haberstroh, K.M., Nauman, E.A., Webster, T.J. Decreased fibroblast and increased osteoblast adhesion on nanostructured NaOH-etched PLGA scaffolds. Int J Nanomed **2**, 383, 2007.
45. Anderson, J.M. The cellular cascades of wound healing. In: Davies, J.E., ed. Bone engineering. Toronto, Cananda: em squared incorporated, 2000, pp. 81–93.
46. Thomsen, P., Esposito, M., Gretzer, C., Liao, H. Inflammatory response to implanted materials. In: Davies, J.E., ed. Bone Engineering. Toronto, Cananda: em squared incorporated, 2000, pp. 118–136.
47. Kukubo, T., Kim, H.M., Kawashita, M., Nakamura, T. What kinds of materials exhibit bone-bonding? In: Davies, J.E, ed. Bone Engineering. Toronto, Cananda: em squared incorporated, 2000, pp. 190–194.
48. Lampin, M., Warocquier-Clerout, R., Legris, C., Degrange, M., Sigot-Luizard, M.F. Correlation between substratum roughness and wettability, cell adhesion, and cell migration. J Biomed Mater Res **36**, 99, 1997.
49. Deligianni, D.D., Katsala, N., Ladas, S., Sotiropoulou, D., Amedee, J., Missirlis, Y.F. Effect of surface roughness of the titanium alloy Ti-6Al-4V on human bone marrow cell response and on protein adsorption. Biomaterials **22**, 1241, 2001.
50. Ponsonnet, L., Reybier, K., Jaffrezic, N., Comte, V., Lagneaub, C., Lissac, M., Martelet, C. Relationship between surface properties (roughness, wettability) of titanium and titanium alloys and cell behaviour. Mater Sci Eng C **23**, 551, 2003.
51. Deligianni, D.D., Katsala, N.D., Koutsoukos, P.G., Missirlis, Y.F. Effect of surface roughness of hydroxyapatite on human bone marrow cell adhesion, proliferation, differentiation and detachment strength. Biomaterials **22**, 87, 2001.
52. Boyan, B.D., Schwartz, Z. Modulation of osteogenesis via implant surface design. In: Davies, J.E., ed. Bone Engineering. Toronto, Cananda: em squared incorporated, 2000, pp. 232–239.

53. Chen, J., Mwenifumbo, S., Langhammer, C., McGovern, J.-P., Li, M., Beye, A., Soboyejo, W.O. Cell/surface interactions and adhesion on Ti-6Al-4V: effects of surface texture. J Biomed Mater Res B Appl Biomater **82B**, 360, 2007.
54. Postiglione, L., Domenico, G.D., Ramaglia, L., Montagnani, S., Salzano, S., Meglio, F.D., Sbordone, L., Vitale, M., Rossi, G. Behavior of SaOS-2 cells cultured on different titanium surfaces. J Dent Res **82**, 692, 2003.
55. Saldana, L., Gonzalez-Carrasco, J.L, Rodriguez, M., Munuera, L., Vilaboa, N. Osteoblast response to plasma-spray porous Ti6Al4V coating on substrates of identical alloy. J Biomed Mater Res **77A**, 608, 2006.

Address correspondence to:
Yuncang Li, Ph.D.
Institute for Technology Research and Innovation
Deakin University
Geelong, Victoria 3217
Australia

E-mail: yuncang.li@deakin.edu.au

Received: March 5, 2009
Accepted: April 7, 2009
Online Publication Date: May 29, 2009